



### **Science Arts & Métiers (SAM)**

is an open access repository that collects the work of Arts et Métiers Institute of Technology researchers and makes it freely available over the web where possible.

This is an author-deposited version published in: <https://sam.ensam.eu>  
Handle ID: <http://hdl.handle.net/10985/15178>

#### **To cite this version :**

Mohamed EL MANSORI, Faissal CHEGDANI - Mechanics of material removal when cutting natural fiber reinforced thermoplastic composites - Polymer Testing - Vol. 67, p.275-283 - 2018

Any correspondence concerning this service should be sent to the repository

Administrator : [scienceouverte@ensam.eu](mailto:scienceouverte@ensam.eu)



# Mechanics of material removal when cutting natural fiber reinforced thermoplastic composites

Faissal Chegdani\*, Mohamed El Mansori

Arts et Métiers ParisTech, MSMP/EA7350, Rue Saint Dominique, BP508, 51006, Châlons-en-Champagne, France

## ARTICLE INFO

### Keywords:

Natural fibers  
Thermoplastic composites  
Machining process  
Mechanical testing  
Chip formation  
Multiscale surface analysis

## ABSTRACT

This paper aims to study the machinability of natural fiber reinforced thermoplastic composites by investigating the mechanics of chip formation and the multiscale cut surface's quality induced by the orthogonal cutting process. Unidirectional flax fibers reinforced polypropylene (UDF/PP) composite has been tested by orthogonal cutting experiments. Mechanical tensile and shear tests have been conducted on UDF/PP specimens to relate the mechanical behavior to the cutting behavior.

Results show that UDF/PP composites produce a continuous chip at all the considered cutting conditions. This is inherently related to the specific mechanical behavior of flax fibers inside the thermoplastic matrix under cutting solicitations. The cutting behavior induces a consequent surface damages in the form of debonding zones and uncut fiber extremities. Results demonstrate that the cutting depth has the most significant influence on the machinability after sorting the pertinent scales of the cut surface using the multiscale surface analysis approach.

## 1. Introduction

The use of natural fiber reinforced plastics (NFRP) composites is becoming an industrial reality, especially in automotive and aerospace industries. NFRP composites are becoming a viable alternative to synthetic fiber composites in many industrial applications that not require high structural performances. This strong industrial demand for NFRP materials is due to the mechanical, economic and ecological benefits that provide natural fibers for sustainable development, particularly plant fibers [1–4]. NFRP composites have aroused the interest of scientists to understand and optimize their manufacturing processes [5–7] and also to investigate their biodegradable behavior [8]. However, the finishing processes have not been well investigated even if few empirical works show that the cutting behavior of plant fiber composites is not the same like that of synthetic fibers [9–12].

Standard machining processes, such as milling, are still the best suitable for machining polymeric composites since they induce low levels of damage in the machined surface [13]. For these reasons, many work was conducted by the authors in order to understand the behavior of plant fibers inside the composite during the industrial machining process of profile milling [14–17]. These studies show that, effectively, the behavior of plant fibers is different from that of synthetic fibers and this is due to their complex and multiscale cellulosic structure around the fiber axis [18]. This structure induces a high transversal elasticity to the plant fiber inside the composite and gives them the ability to deform

easily, which makes there shearing difficult during the cutting process. The previous author's works show also that investigating the machined surfaces of NFRP composites requires the selection of the relevant scales that allow the discrimination of both material and process parameters effects. Indeed, unlike glass fibers, plant fibers present a scale effect since their mechanical properties depends on the mechanical scale used for the analysis as demonstrated in Ref. [19].

Nowadays, the use of natural fiber composites is focused also on structural applications that require high mechanical performances, especially long plant fiber reinforced polymer composites [4,20–22]. In the context of sustainable development and circular economy, the interest is oriented toward the thermoplastic composites because thermoplastic matrices are recyclable. Thus, since the mechanical properties of thermoplastic composites are lower than that of thermoset composites, it is necessary to understand the relationship between the mechanical properties of plant fibers reinforced thermoplastic composites and their mechanics of cutting in order to optimize their manufacturing processes and avoid mechanical cutting-induced damages.

In this paper, the fundamental process of orthogonal cutting is conducted on unidirectional flax fibers reinforced polypropylene (UDF/PP) composites in order to investigate the chip formation mechanisms. Mechanical tensile and shear tests are realized on the same material for better comprehension of the cutting process from a mechanical point of view.

The induced machined surfaces are evaluated by scanning electron

\* Corresponding author.

E-mail address: faissal.chegdani@ensam.eu (F. Chegdani).

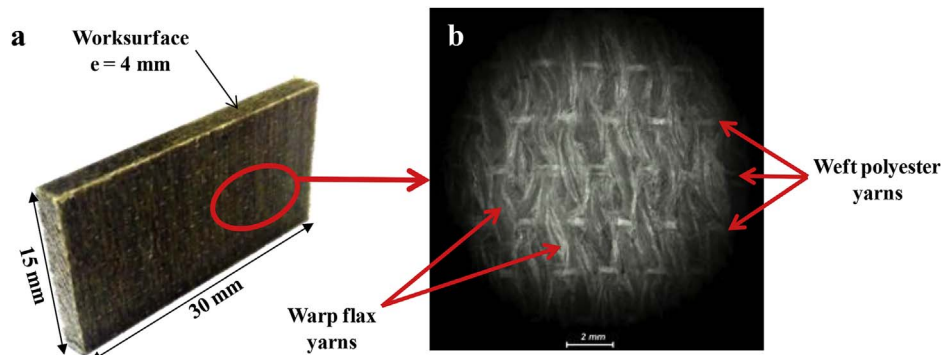


Fig. 1. a) UDF/PP workpiece. b) Fibrous structure of flax fibers reinforcement.

microscopy (SEM). Then, cutting forces are plotted to show the influence of each process parameter on the cutting operation. The machined surfaces topography is investigated by a multiscale approach based on discrete wavelet transform. Statistical analysis of variance (ANOVA) is realized at the end to quantify the contribution rate of each process parameter on the multiscale roughness of the machined surfaces.

## 2. Material and methods

### 2.1. Unidirectional flax/polypropylene composite workpieces

Unidirectional flax fiber composites used in this study (Fig. 1(a)) are supplied by "Composite Evolution - UK". The composite structure is produced by unidirectional long flax fibers (UDF) and polypropylene matrix (PP) as continuous warp flax yarns. Synthetic weft yarns assure the unidirectionality of the composite. The flax/PP composition is 40% *vt* of UDF and 60% *vt* of PP (approximately 50% *wt* for each constituent). The warp yarn diameter is approximately 1 mm (Fig. 1(b)). The weft yarns are composed of co-polyamide/polyester co-spun. The incidence of weft yarns is 1 yarn per 2.5 mm, giving an areal weight of 14 g/m<sup>2</sup> (approximately 5% of the total fabric). Table 1 summarizes the mechanical properties of flax fibers and PP matrix. The supplier provides these technical data.

Inside each flax yarn, the distribution of the elementary flax fibers is random in terms of geometry (cylindrical to polygonal), size (10 μm–20 μm) and location as shown in Fig. 2(a). Some elementary fibers are thus gathered into a bundle, which called technical fiber (Fig. 2(b)), and other elementary fibers are isolated in the matrix. This random distribution can have an influence on characterizing the machined surfaces of UDF/PP composites.

### 2.2. Mechanical tests

Tensile tests (Fig. 3(a)) have been performed on Instron 4482 Universal testing machine according to ISO-527 standard. The in-situ strain of the tested UDF/PP samples has been recorded by Instron 2630-100 Clip-on extensometer. Shear tests have been realized using the Iosipescu method showed in Fig. 3(b) and described in Refs. [23,24]. The in-situ strain of the Iosipescu specimens has been measured by VPG Tee Rosettes gages (Model CEA-06-032WT). Tensile and shear tests have been realized for different displacement speeds.

Table 1  
Mechanical properties flax fibers and PP matrix used in composite workpieces.

	Flax fiber	PP matrix
Tensile modulus (GPa)	50	0.93
Tensile strength (MPa)	500	29.5
Maximum strain	2%	14%

### 2.3. Cutting tests

Orthogonal cutting experiments, as shown in Fig. 4, were conducted on a shaper machine (model GSP-EL 136). The machine is of maximum power of 5222 W, maximum stroke of 650 mm and maximum speed of 100 m min<sup>-1</sup>. Three cutting inserts supplied by "Sandvik Coromant – FR" (A4F3, A4BQ and A4BS) have a unique cutting geometry with 20° rake angle and 7° clearance angle. The main objective for adding coating film is to increase the cutting edge radius as shown in Table 2.

Tests were performed under dry conditions. The specimen was clamped manually in the machine bearing between two hard steel plates as shown in Fig. 4. Edge trimming of the composite material results from the relative motion between the tool, fixed to the moving saddle, and the specimen. The fibers orientation is always perpendicular to the cutting direction in order to consider the worst cutting condition. For getting reliable results, each test was repeated three times under identical conditions and with a new cutting insert at each time. Table 3 summarizes the cutting conditions considered in this study.

### 2.4. Experimental measurements

To highlight the in-situ chip formation mechanisms during cutting, a fast-camera (FASTCAM SA5 CCD) was used for recording optical frames at an acquisition rate of 20,000 fps. The in-situ cutting forces have been recorded using a piezoelectric Kistler dynamometer (model 9255B), connected to a multichannel charge amplifier (model 5019 B131) and a data acquisition board. The considered cutting force is the measured component that is parallel to the cutting direction.

Microscopic observations of UDF/PP machined surfaces state were made by scanning electron microscope (SEM) (JSM –5510LV) at low vacuum mode. Typical representative surface morphology as induced by machining of each experimental configuration was considered for the microscopic analysis. Geometrical and superficial variations of each workpiece samples have been measured at five locations using a 2D Surfscan stylus profilometer according to the ISO-4287 standard. The tip radius of the diamond stylus is 2 μm. The surface profile on each specimen was taken along the machining direction over a sampling length of 8 μm. The evaluation length is 16.8 mm and a cut-off of 0.8 mm is used to apply the multiscale decomposition of the overall topography signal by discrete wavelet transform [25].

## 3. Results and discussion

### 3.1. Mechanical behavior of UDF/PP specimens

Fig. 5 presents both tensile and shear behaviors of UDF/PP specimens for different deformation speeds. Tensile behavior shows two linear parts (Fig. 5(a)), the first part corresponds to the contribution of the fibrous reinforcement and the polymer matrix. By reaching a stress

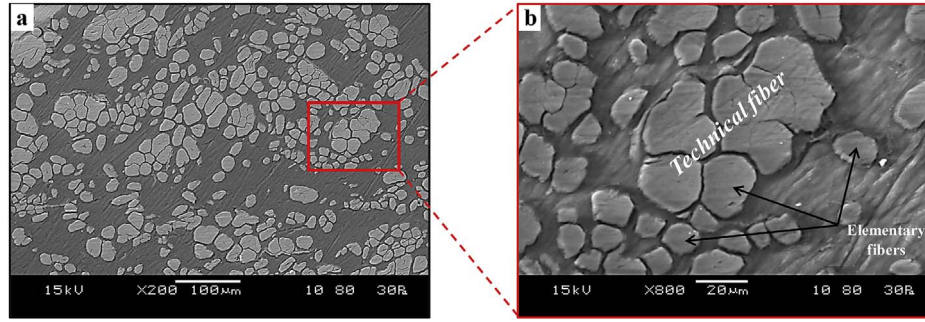


Fig. 2. a) SEM image of the flax fibers distribution in the composite. b) SEM image of the technical fiber.

value of 30 MPa (i.e. the tensile strength of PP matrix), the behavior remains linear but the stiffness decreases due to debonding between fibers and matrix. At a stress value of approximately 100 MPa, the behavior becomes nonlinear, corresponding to a plastic behavior until break (Fig. 6(a)). Thus, the UDF/PP composites have a linear tensile behavior with ductile break and the effect of displacement speed is only apparent on the plastic zone that increases the strain at break.

The shear curves of UDF/PP specimens show an elastoplastic behavior (Fig. 5(b)). The increasing of displacement speed increases the shear modulus but does not have an influence on the ductile shear behavior. It's important to mention that the break has not been reached by the Iosipescu test. Indeed, throughout the loading, the fibers follow the movement of shear and deform transversely with a debonding between the fibers and matrix that is observed during the deformation at the shear zone (Fig. 6(c)). The fibers continue to deform until be mainly under tensile solicitation.

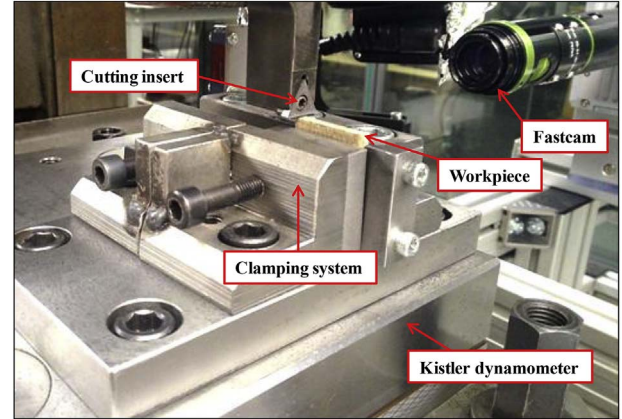


Fig. 4. Experimental setup of the orthogonal cutting tests.

### 3.2. Chip formation of UDF/PP composites

Fig. 7 shows the in-situ chip morphology for different cutting conditions. Both cutting speed and depth influence the chip curling. Cutting UDF/PP samples with low cutting speed and low cutting depth favors the chip curling (Fig. 7(a)). Increasing these two parameters reduces the chip curling due to the increase of plastic deformation resistance in the UDF/PP workpieces (Fig. 7(i)). Reducing the chip curling can have an impact on the tribological contact behavior between the cutting tool and the NFRP material. Indeed, when the chip curling is reduced, there is more contact between the removed chip and the tool rake face, which increases the friction at this contact area. Therefore, reducing the chip curling can accelerate the tool wear.

The fast-cam images of Fig. 7 show that, regardless of cutting speed and depth at the considered values range, the UDF/PP composite generates a continuous long chip on all the cutting length for all the cutting conditions. This finding is specifically different from that of synthetic

Table 2

Coating characteristics of each cutting insert.

Reference	A4F3	A4BQ	A4BS
Substrate	WC	WC	WC
Coating process	–	Multilayer CVD	Multilayer CVD
Coating composition	–	Diamond sp <sup>3</sup>	Diamond sp <sup>3</sup>
Hardness (HV)	1600	10000	10000
Coating thickness (μm)	–	9 ± 1	14 ± 2
Cutting edge radius (μm)	12 ± 1.7	21 ± 1.5	27 ± 2

fiber composites as glass or carbon fibers. Indeed, the chip formation of synthetic fiber composites depends on the matrix nature. For thermoset composites, the removed chip is often discontinuous or powdery [26–35]. This is inherently related to the mechanical behavior of the thermoset composite during the cutting solicitations. This mechanical behavior is similar to shearing solicitations that show a brittle behavior

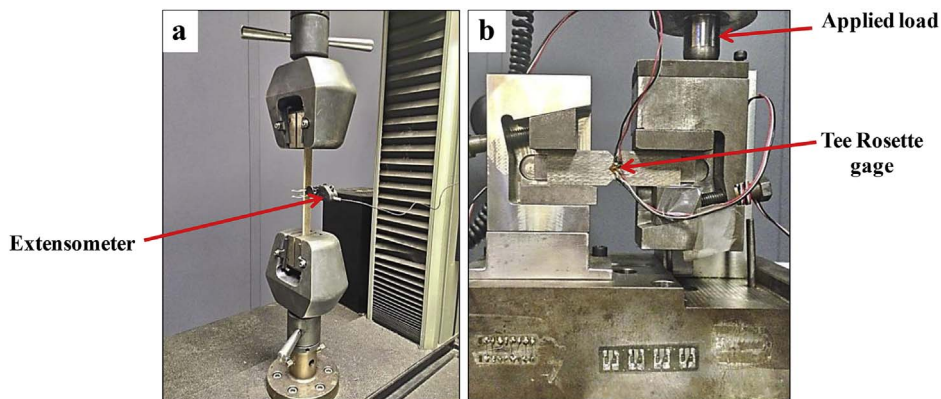


Fig. 3. a) ISO-527 tensile test. b) Iosipescu shear test.



**Table 3**  
Process parameters used for the orthogonal cutting tests.

Cutting inserts	Cutting speed (m/min)	Depth of cut ( $\mu\text{m}$ )
A4F3	12	100
A4BQ	20	300
A4BS	32	500
	50	
	80	

using Iosipescu shear tests [24,36]. On the other side, the chip formation of synthetic fiber reinforced thermoplastic composites tend to be continuous [37–40], except for high cutting speed where the removed chip becomes discontinuous [40]. This demonstrates that the matrix nature has a significant role in the chip formation. Thermosetting matrix is brittle and its cutting mechanism is dominated by fracture, while thermoplastic matrix has the capability to withstand large elastic and plastic strains. However, the continuous-to-discontinuous chip transition has been reported to occur for general synthetic fiber composites when the fibers orientation is above  $75^\circ$  and near to  $90^\circ$ . This is because of the severity of interlaminar shear. This transition is marked by the change in direction of the force parallel to the fibers from tensile to compressive, which makes the fibers shearing more difficult [41,42].

In the case of UDF/PP composites, the mechanical behaviors are different as explained in Section 3.1. Flax fiber composites show a ductile behavior at both tensile and shear tests. At Iosipescu shear test, which the solicitations can be similar to those of the cutting operation, the ductile behavior is followed by a transverse deformation of flax fibers toward the shear direction. This is because flax fibers have a high transverse flexibility due to the microstructure of cellulosic microfibrils that are oriented along the fiber axis [17,18]. The flax stiffness is then intensive on the fiber axis direction and the transverse stiffness is significantly low. The cutting contact stiffness is thus low and flax fibers follow the deformation movement of the PP matrix during the cutting operation. Then, the cohesion between fibers and matrix can withstand the stresses of the cutting operation and, consequently, the removed chip remains continuous.

### 3.3. Cutting forces

Fig. 8 presents the cutting forces on the orthogonal cutting direction. It can be seen a drastic increasing of cutting force by cutting depth increase. Increasing the cutting speed increases the cutting forces. However, increasing either the cutting depth or the cutting edge radius reduces the impact of the cutting speed. Therefore, the effect of the cutting speed becomes insignificant when cutting by an edge radius of  $27\mu\text{m}$  with  $500\mu\text{m}$  of cutting depth.

Increasing either the cutting depth or the cutting speed increases the

cutting forces by raising the material removal rate. However, the cutting depth effect is more significant because it increases the chip thickness that enhances the material resistance when cutting. On the other side, the cutting speed has a double effect. Indeed, increasing the cutting speed increases the material removal rate and then the cutting forces. Nevertheless, cutting speed growing induces high temperatures at the cutting zone that makes the material softer and leads to reduce the cutting forces. Therefore, the thermal effect compensates the material removal rate effect. This thermal effect is also induced by the cutting depth and the edge radius of the cutting tool. In fact, increasing the cutting depth increases plastic deformations when cutting and, then, the material temperature is growing due to high plastic deformation rates. The cutting edge radius increase leads to raise the cutting contact area which favors the temperature increase at the cutting zone due to friction. All these physical phenomena can explain why the effect of cutting speed is reduced at both high cutting depth and edge radius.

Cutting forces analysis shows the significance of the cutting depth to control the machinability of flax fiber composites because increasing the cutting depth by  $200\mu\text{m}$  can considerably increase the cutting force and, consequently, this will cause bulk and surface damages. Next section deals with the study of these damages.

### 3.4. Microscopic quality of machined surfaces

Fig. 9 presents the SEM images of machined surfaces at the same cutting speed ( $80\text{ m/min}$ ) for different cutting conditions. Cutting UDF/PP composites with  $12\mu\text{m}$  of edge radius and  $100\mu\text{m}$  of cutting depth generates efficient fibers shearing because flax fibers cross-sections can be observed in Fig. 9(a). By increasing the cutting edge radius, plastic deformation of flax fibers cross-sections can be noticed in Fig. 9(d) and (g). Indeed, fibers cross-sections shape is changed when growing from higher to lower tool sharpness. Increasing the cutting edge radius increases the fibers cross-sections diameter by plastic deformation of these latter. On the other side, increasing the cutting depth deteriorates the fibers shearing where flax fibers are transversely deformed toward the cutting direction before being sheared. This induced some uncut fiber extremities that remain on the machined surface (Fig. 9(c)). Increasing the depth of cut increases not only the uncut fiber extremities but also the debonding zones between elementary fibers and PP matrix, especially when it is associated with a cutting edge radius increase (Fig. 9(i)).

The uncut fiber extremities are the specific phenomena in the case of machining plant fiber composites because of the transverse flexibility issue of plant fibers when being in contact with the cutting tool as demonstrated in the previous milling operation work [15–17], especially when increasing the cutting edge radius [17]. Moreover, the high cutting forces induced by increasing the cutting depth (Fig. 8) causes more failure of the interfaces between elementary flax fibers and PP

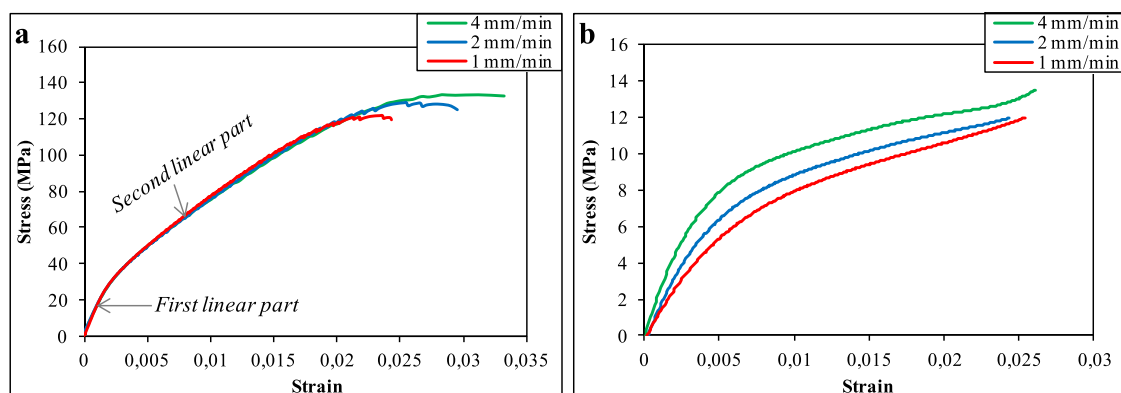


Fig. 5. A typical behavior curves of UDF/PP composites at different displacement speeds. a) Tensile test. b) Iosipescu shear test.

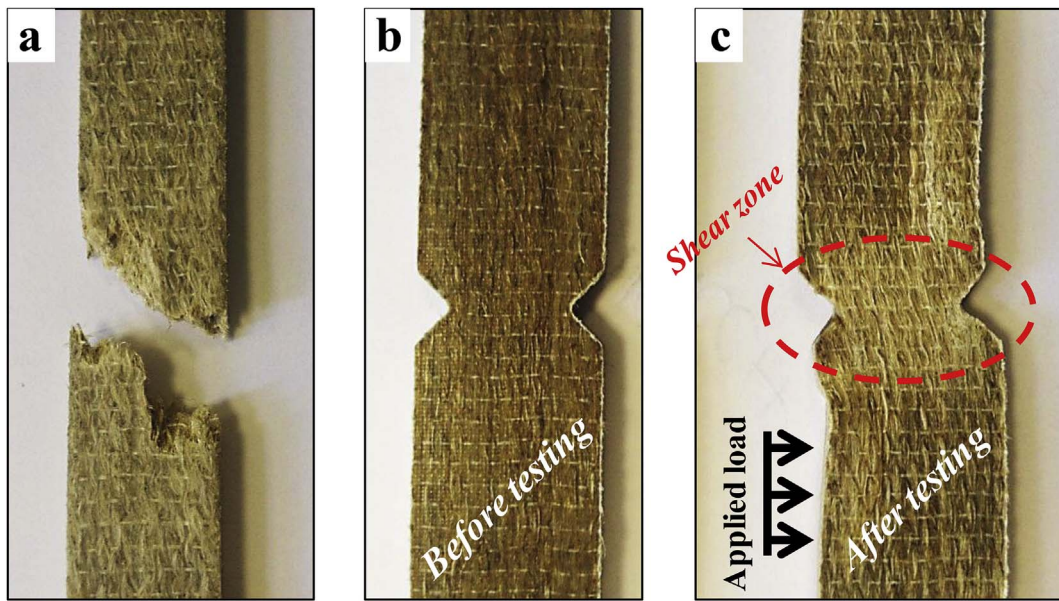


Fig. 6. a) Tensile specimen after break. b) Iosipescu specimen before shear test. c) Iosipescu specimen after shear test.

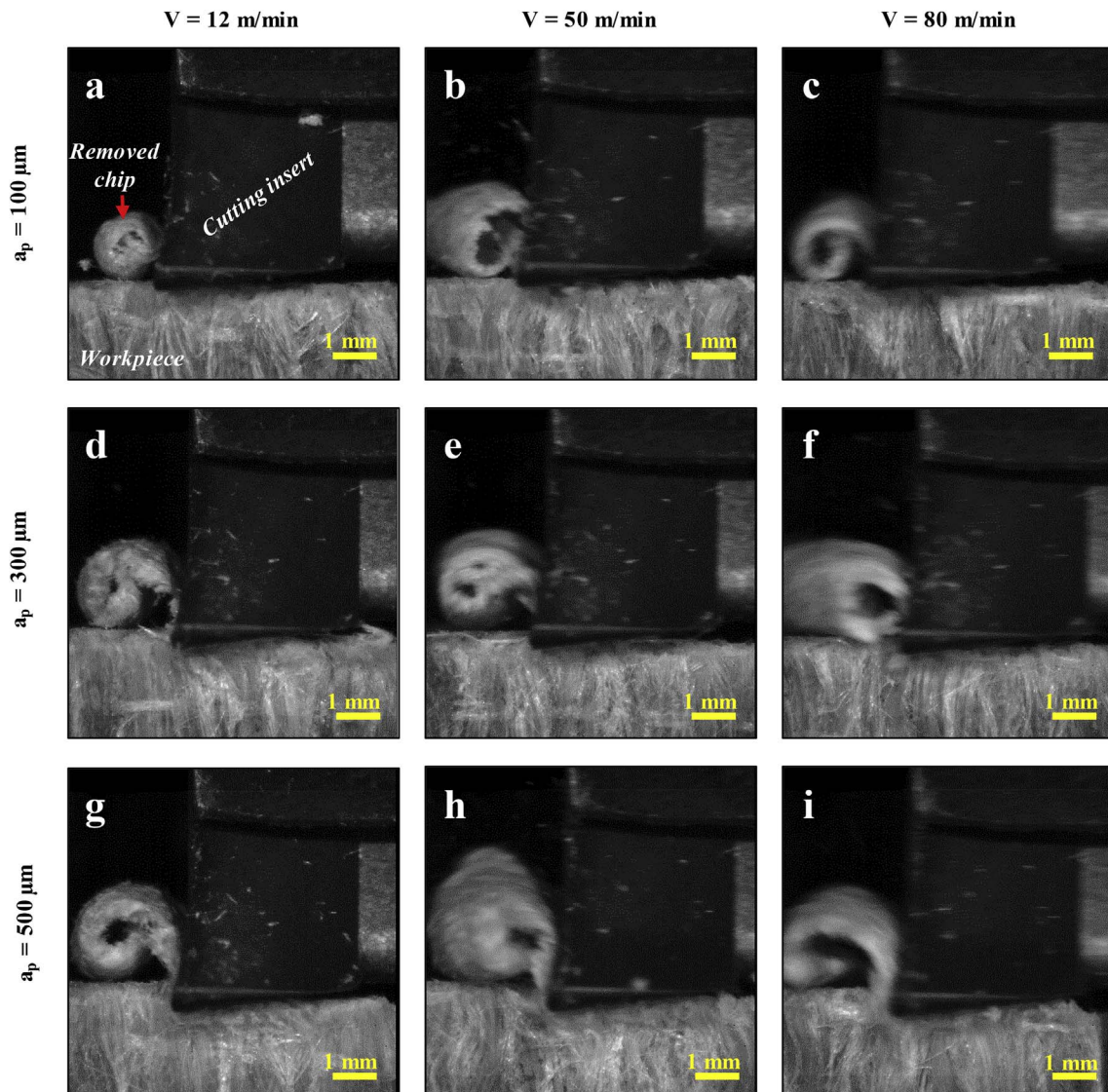


Fig. 7. Fast-cam images showing the chip formation for different cutting speeds ( $V$ ) and depths ( $a_p$ ) using  $r_c = 27 \mu\text{m}$ .



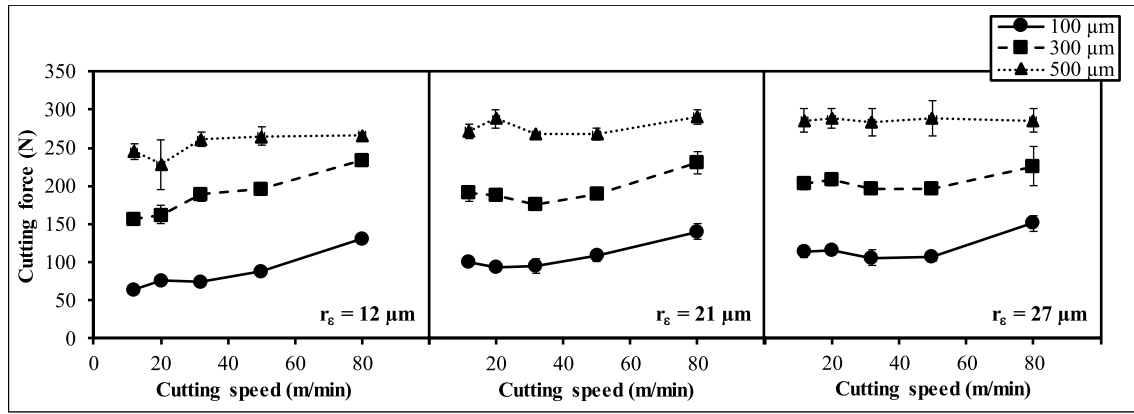


Fig. 8. Induced cutting forces during cutting operations for all cutting conditions.

matrix and this will reduce the cutting contact stiffness. Consequently, more deformation will be produced when the cutting contact which makes difficult the fiber shearing during the cutting operation. On another side, and unlike synthetic fibers of glass or carbon, natural fibers are known as composite materials of cellulose microfibrils embedded in amorphous natural polymers of hemicellulose and lignin [14,18]. The amorphous component of natural fibers allows plastic deformations of these latter, especially when increasing the temperature during the cutting process since the fibers will be softer and easily able to deform.

### 3.5. Multiscale surface roughness of machined surfaces

The multiscale discrete wavelet transform (DWT) approach [15,17] consists on decomposing the global topographic signal through a series

of high-pass and low-pass filters to analyze the high and low frequencies [43]. Since the high frequencies correspond to the micro-roughness and the low frequencies correspond to the waviness, it can be obtained, after reconstruction, the multiscale spectrum that reveals the mean arithmetic roughness “Ma(i)” at each scale “i” of the decomposition [44].

Fig. 10 presents the evolution of the multiscale spectrums at cutting speed  $V = 20 \text{ m/min}$  for the different cutting edge radius. Globally, the roughness increases by the scale increasing. The multiscale approach can discriminate the cutting depth effect at the mesoscopic scales between  $50 \mu\text{m}$  and  $1 \text{ mm}$ . Then, the relevant scales are those of the fibrous structure size inside the composite (i.e. from technical fiber size [ $\sim 50 \mu\text{m}$ ] to fiber yarn size [ $\sim 1 \text{ mm}$ ]). This finding corresponds to the conclusions obtained by profile milling process [15–17]. However, for

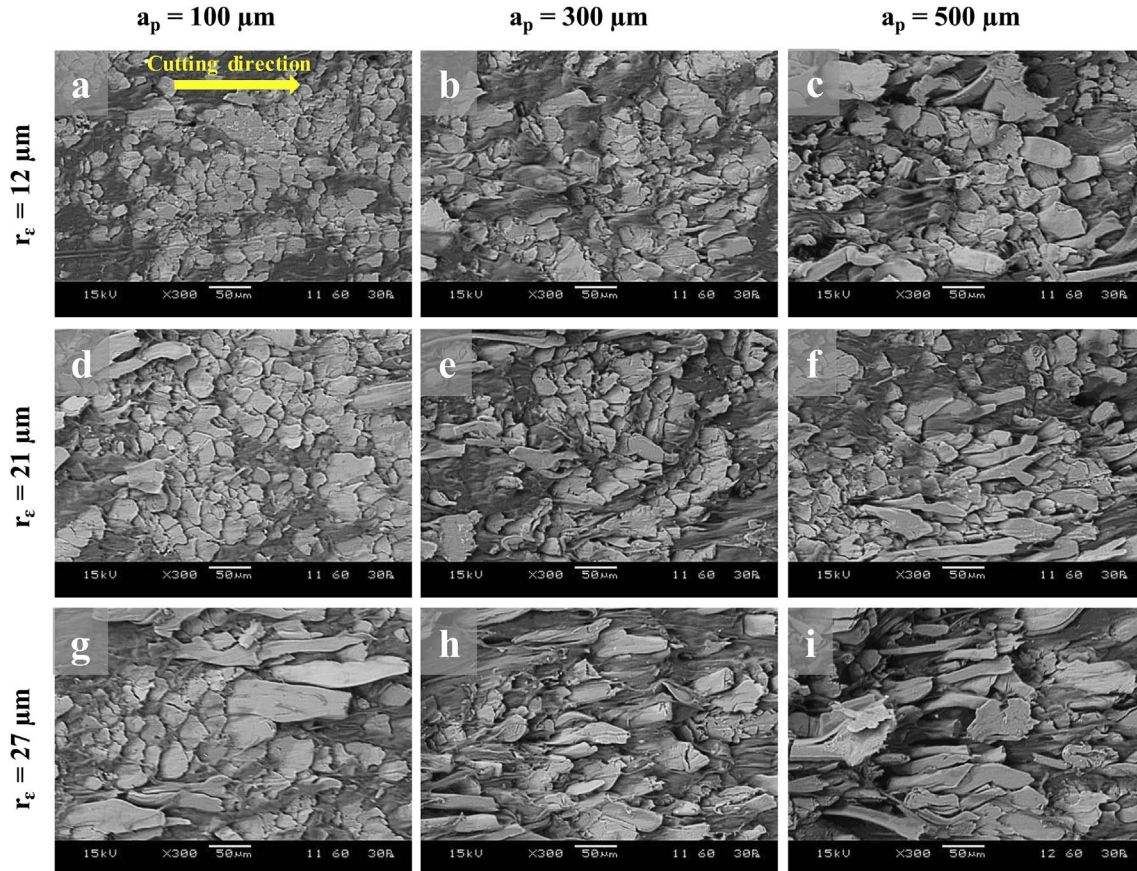


Fig. 9. SEM images of microscopic surfaces quality for different cutting edge radius ( $r_e$ ) and cutting depth ( $a_p$ ).

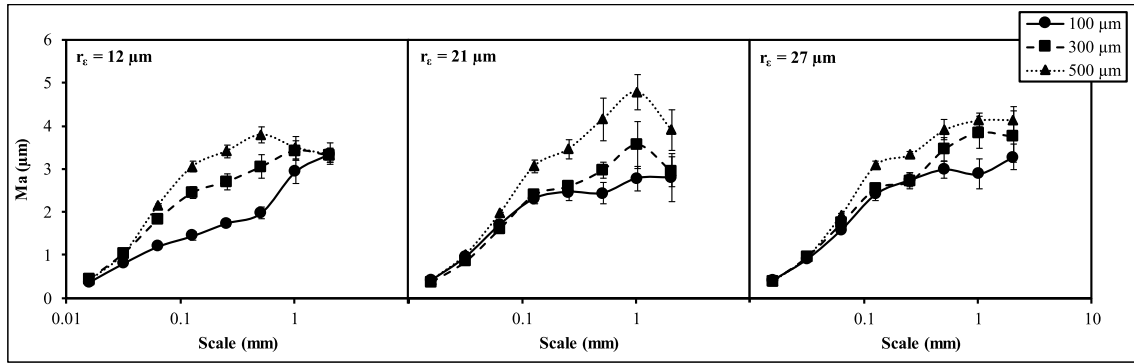


Fig. 10. Multiscale surface roughness spectrums drawn at each cutting depth for the different cutting edges radius at cutting speed  $V = 20$  m/min.

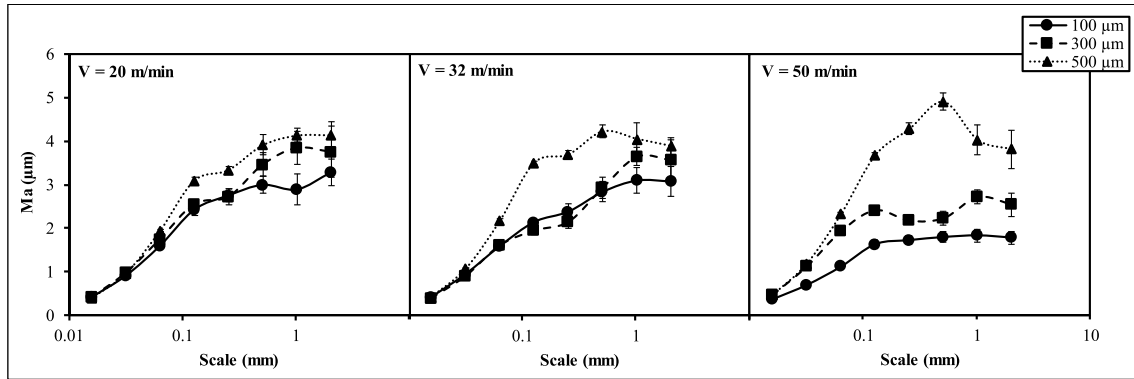


Fig. 11. Multiscale surface roughness spectrums drawn at each cutting depth for different cutting speeds at the cutting edge radius  $r_e = 27$  μm.

the orthogonal cutting process, it can be seen in Fig. 10 that increasing the cutting edge radius reduces the relevant scales toward the macroscopic scales by increasing the cutting contact area as demonstrated in Ref. [45].

Fig. 11 shows the effect of cutting speed on the multiscale surface roughness spectrums for the cutting edge radius  $r_e = 27$  μm. Increasing the cutting speed increases the relevant scales range that allow the discrimination of the cutting speed effect. At the relevant scales, the multiscale spectrums of Fig. 11 show that the effect of cutting speed is more obvious at the low cutting depth. Increasing the cutting speed decreases the surface roughness except for a cutting depth of 500 μm where the cutting speed is not highly significant. Indeed, increasing the cutting speed increases the shear modulus (Fig. 5(b)) which will increase the contact stiffness and, then, the shearing efficiency.

### 3.6. Multiscale contribution rate of process parameters to the surface quality

To quantify the contribution of the studied process parameters, ANOVA [46,47] of input variables influence has been performed at each multiscale response of surface quality (i.e. at each scale “ $p$ ” of the decomposition) using XLSTAT software. The contribution ratio of each “ $\alpha$ ” factor ( $C_\alpha$ ) was calculated with the Fisher criterion test ( $F(\alpha)$ ) at the correlation coefficient ( $R^2$ ) confidence [46,48]. Eq. (1) can define the contribution ratio of each factor. More explanations about this statistical technique are in Ref. [14].

$$C_\alpha = \frac{F(\alpha)}{\sum_{\alpha} F(\alpha)} \times R^2 \quad (1)$$

Fig. 12 presents the contribution rate of each process parameter at each analysis scale. It can be seen the low contribution of the cutting edge radius regarding the other parameters until the macroscopic scales. The behavior of the multiscale contribution rate confirms the previous results. Indeed, Fig. 12 shows the significant impact of cutting

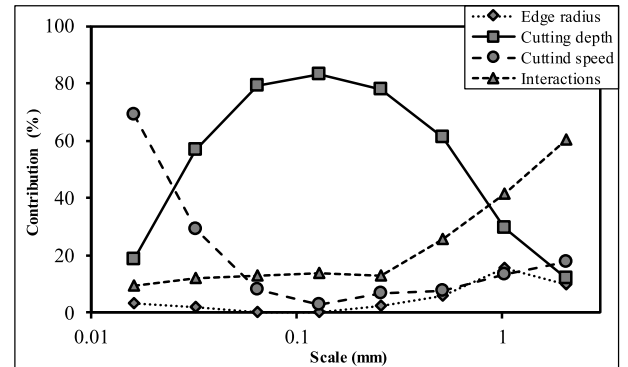


Fig. 12. Multiscale contribution rate of each process parameter.

depth at the relevant scale (i.e. mesoscopic scale) identified in Section 3.5. At macroscopic scale, the random distribution of technical fibers seen in Fig. 2 influences the contribution of the process parameters and increases the interactions between them. Then, the interactions have the predominant contribution.

## 4. Conclusions

Orthogonal cutting process has been conducted on unidirectional flax fiber reinforced polypropylene (UDF/PP) composites in order to investigate the mechanics of material removal by realizing mechanical tests on the same material. The resulting machined surfaces have been evaluated by SEM observations and multiscale topographic analysis. The following conclusions can be drawn:

- Even if flax fibers are oriented perpendicularly to the cutting direction, UDF/PP composites show a long continuous chip during the orthogonal cutting process at a large range of cutting speed and



depth values. This chip behavior is different from that of synthetic thermoplastic composites, which have a discontinuous chip at dry and high loading cutting conditions.

- The specific cutting behavior of UDF/PP composites is related to the mechanical ductile behavior of the thermoplastic matrix combined with the high transverse elasticity of flax fibers that have also a ductile behavior unlike glass or carbon fibers.
- The cutting depth has the greatest influence on machined surface state. Increasing the cutting depth increases the cutting forces and, then, the surface damages in form of debonding zones, uncut fibers extremities and plastic deformation of flax fibers on the machined surface. The effect of cutting speed is significantly reduced due to the thermal effect induced by friction and plastic deformation.
- Analyzing the machined surfaces of flax fiber composites requires the selection of the relevant scales. The effects of both cutting depth and cutting edge radius are more obvious at the scales that correspond to the flax fibrous structure size inside the composite. ANOVA analysis confirms that the cutting depth is strongly the most influent parameter on the machined surface quality at the relevant scales.

## Acknowledgements

The authors acknowledge the urban community of Châlons-en-Champagne (*Cités en Champagne*) for their financial support.

## References

- [1] D.B. Dittenber, H.V.S. GangaRao, Critical review of recent publications on use of natural composites in infrastructure, *Compos. Part A Appl. Sci. Manuf* 43 (2012) 1419–1429, <http://dx.doi.org/10.1016/j.compositesa.2011.11.019>.
- [2] O. Faruk, A.K. Bledzki, H.-P. Fink, M. Sain, Biocomposites reinforced with natural fibers: 2000–2010, *Prog. Polym. Sci.* 37 (2012) 1552–1596, <http://dx.doi.org/10.1016/j.progpolymsci.2012.04.003>.
- [3] A. Lefevre, A. Bourmaud, C. Morvan, C. Balev, Tensile properties of elementary fibres of flax and glass: analysis of reproducibility and scattering, *Mater. Lett.* 130 (2014) 289–291, <http://dx.doi.org/10.1016/j.matlet.2014.05.115>.
- [4] D.U. Shah, Developing plant fibre composites for structural applications by optimising composite parameters: a critical review, *J. Mater. Sci.* 48 (2013) 6083–6107, <http://dx.doi.org/10.1007/s10853-013-7458-7>.
- [5] K. Sam-Jung, M. Jin-Bok, K. Gue-Hyun, kHa Chang-Si, Mechanical properties of polypropylene/natural fiber composites: comparison of wood fiber and cotton fiber, *Polym. Test.* 27 (2008) 801–806, <http://dx.doi.org/10.1016/J.POLYMERTESTING.2008.06.002>.
- [6] M. Nasihatgozar, V. Daghighi, T. E. Lacy Jr., H. Daghighi, K. Nikbin, A. Simoneau, Mechanical characterization of novel latania natural fiber reinforced PP/EPDM composites, *Polym. Test.* 56 (2016) 321–328, <http://dx.doi.org/10.1016/J.POLYMERTESTING.2016.10.016>.
- [7] A. Shalwan, B.F. Yousif, State of Art: mechanical and tribological behaviour of polymeric composites based on natural fibres, *Mater. Des.* 48 (2013) 14–24, <http://dx.doi.org/10.1016/j.matdes.2012.07.014>.
- [8] A.G. Michael, M.G. Luke, A.K. John, G.L. John, L.H. Clement, Mechanical and biodegradation performance of short natural fibre polyhydroxybutyrate composites, *Polym. Test.* 32 (2013) 1603–1611, <http://dx.doi.org/10.1016/J.POLYMERTESTING.2013.10.011>.
- [9] P.N.E. Naveen, M. Yasaswi, R.V. Prasad, Experimental investigation of drilling parameters on composite materials, *J. Mech. Civ. Eng* 2 (2012) 30–37.
- [10] L.M.P. Durão, D.J.S. Gonçalves, J.M.R.S. Tavares, V.H.C. de Albuquerque, T.H. Panzera, L.J. Silva, A. A. Vieira, A. P.M. Baptista, Drilling delamination outcomes on glass and sisal reinforced plastics, *Mater. Sci. Forum* 730–732 (2012) 301–306, <http://dx.doi.org/10.4028/www.scientific.net/MSF.730-732.301>.
- [11] P.K. Bajpai, K. Debnath, I. Singh, Hole making in natural fiber-reinforced polyactic acid laminates, *J. Thermoplast. Compos. Mater.* 30 (2017) 30–46, <http://dx.doi.org/10.1177/0892705715575094>.
- [12] G.D. Babu, K.S. Babu, B.U.M. Gowd, Effect of machining parameters on milled natural fiber-reinforced plastic composites, *J. Adv. Mech. Eng* (2013) 1–12, <http://dx.doi.org/10.7726/jame.2013.1001>.
- [13] A. Codoloni, Q.M. Li, A. Wilkinson, Influence of machining process on the mechanical behaviour of injection-moulded specimens of talc-filled Polypropylene, *Polym. Test* 62 (2017) 342–347, <http://dx.doi.org/10.1016/J.POLYMERTESTING.2017.07.018>.
- [14] F. Chegdani, S. Mezghani, M. El Mansori, Correlation between mechanical scales and analysis scales of topographic signals under milling process of natural fibre composites, *J. Compos. Mater.* 51 (2017) 2743–2756, <http://dx.doi.org/10.1177/0021998316676625>.
- [15] F. Chegdani, S. Mezghani, M. El Mansori, A. Mkaddem, Fiber type effect on tribological behavior when cutting natural fiber reinforced plastics, *Wear* 332–333 (2015) 772–779, <http://dx.doi.org/10.1016/j.wear.2014.12.039>.
- [16] F. Chegdani, S. Mezghani, M. El Mansori, On the multiscale tribological signatures of the tool helix angle in profile milling of woven flax fiber composites, *Tribol. Int.* 100 (2016) 132–140, <http://dx.doi.org/10.1016/j.triboint.2015.12.014>.
- [17] F. Chegdani, S. Mezghani, M. El Mansori, Experimental study of coated tools effects in dry cutting of natural fiber reinforced plastics, *Surf. Coatings Technol* 284 (2015) 264–272, <http://dx.doi.org/10.1016/j.surfcoat.2015.06.083>.
- [18] C. Balev, Analysis of the flax fibres tensile behaviour and analysis of the tensile stiffness increase, *Compos. - Part A Appl. Sci. Manuf* 33 (2002) 939–948, [http://dx.doi.org/10.1016/S1359-835X\(02\)00040-4](http://dx.doi.org/10.1016/S1359-835X(02)00040-4).
- [19] F. Chegdani, M. El Mansori, S. Mezghani, A. Montagne, Scale effect on tribo-mechanical behavior of vegetal fibers in reinforced bio-composite materials, *Compos. Sci. Technol.* 150 (2017) 87–94, <http://dx.doi.org/10.1016/j.compscitech.2017.07.012>.
- [20] K. Moussa, M. Valérie, D. Arnaud, A. Boussad, A. Fazilay, G. Ying Qiao, V. François, R. Frédéric, Flax/Acrodur® sandwich panel: an innovative eco-material for automotive applications, *JEC Compos. Mag* 51 (2014) 54–59.
- [21] M. Khalfallah, B. Abbès, Y.Q. Guo, V. Marcel, A. Duval, F. Vanfleteren, F. Rousseau, Innovative flax tapes reinforced Acrodur biocomposites: a new alternative for automotive applications, *Mater. Des.* 64 (2014) 116–126, <http://dx.doi.org/10.1016/j.matdes.2014.07.029>.
- [22] G. Koronis, A. Silva, M. Fontul, Green composites: a review of adequate materials for automotive applications, *Compos. Part B Eng* 44 (2013) 120–127, <http://dx.doi.org/10.1016/j.compositesb.2012.07.004>.
- [23] F. Pierron, Saint-venant effects in the Iosipescu specimen, *J. Compos. Mater.* 32 (1998) 1986–2015, <http://dx.doi.org/10.1177/002199839803202201>.
- [24] P. Ghidossi, M. El Mansori, F. Pierron, Ge machining effects on the failure of polymer matrix composite coupons, *Compos. Part A Appl. Sci. Manuf* 35 (2004) 989–999, <http://dx.doi.org/10.1016/j.compositesa.2004.01.015>.
- [25] X. Chen, J. Raja, S. Simanapalli, Multi-scale analysis of engineering surfaces, *Int. J. Mach. Tool Manufact.* 35 (1995) 231–238, [http://dx.doi.org/10.1016/0890-6955\(94\)P2377-R](http://dx.doi.org/10.1016/0890-6955(94)P2377-R).
- [26] A. Ben Soussia, A. Mkaddem, M. El Mansori, Rigorous treatment of dry cutting of FRP – interface consumption concept: a review, *Int. J. Mech. Sci.* 83 (2014) 1–29, <http://dx.doi.org/10.1016/j.jmesci.2014.03.017>.
- [27] N. Bhatnagar, N. Ramakrishnan, N.K. Naik, R. Komanduri, On the machining of fiber reinforced plastic (FRP) composite laminates, *Int. J. Mach. Tool Manufact.* 35 (1995) 701–716, [http://dx.doi.org/10.1016/0890-6955\(95\)93039-9](http://dx.doi.org/10.1016/0890-6955(95)93039-9).
- [28] A. Koplev, A. Lystrup, T. Vorm, The cutting process, chips, and cutting forces in machining CFRP, *Composites* 14 (1983) 371–376, [http://dx.doi.org/10.1016/0010-4361\(83\)90157-X](http://dx.doi.org/10.1016/0010-4361(83)90157-X).
- [29] M. Zimmermann, L. Heberger, F. Schneider, C. Effgen, J.C. Aurich, Investigation of chip formation and workpiece load when machining carbon-fiber-reinforced-polymer (CFRP), *Procedia Manuf* 6 (2016) 124–131, <http://dx.doi.org/10.1016/J.PROMFG.2016.11.016>.
- [30] V. Lopresto, A. Caggiano, R. Teti, High performance cutting of fibre reinforced plastic composite materials, *Procedia CIRP* 46 (2016) 71–82, <http://dx.doi.org/10.1016/J.PROCIR.2016.05.079>.
- [31] F. Kahwash, I. Shyha, A. Maheri, Machining unidirectional composites using single-point tools: analysis of cutting forces, chip formation and surface integrity, *Procedia Eng* 132 (2015) 569–576, <http://dx.doi.org/10.1016/J.PROENG.2015.12.534>.
- [32] H. Li, X. Qin, G. He, Y. Jin, D. Sun, M. Price, Investigation of chip formation and fracture toughness in orthogonal cutting of UD-CFRP, *Int. J. Adv. Manuf. Technol.* 82 (2016) 1079–1088, <http://dx.doi.org/10.1007/s00170-015-7471-x>.
- [33] D. Arola, M. Ramulu, Orthogonal cutting of fiber-reinforced composites: a finite element analysis, *Int. J. Mech. Sci.* 39 (1997) 597–613, [http://dx.doi.org/10.1016/S0020-7403\(96\)00061-6](http://dx.doi.org/10.1016/S0020-7403(96)00061-6).
- [34] D.H. Wang, M. Ramulu, D. Arola, Orthogonal cutting mechanisms of graphite/epoxy composite. Part II: multi-directional laminate, *Int. J. Mach. Tool Manufact.* 35 (1995) 1639–1648, [http://dx.doi.org/10.1016/0890-6955\(95\)00015-P](http://dx.doi.org/10.1016/0890-6955(95)00015-P).
- [35] D.H. Wang, M. Ramulu, D. Arola, Orthogonal cutting mechanisms of graphite/epoxy composite. Part I: unidirectional laminate, *Int. J. Mach. Tool Manufact.* 35 (1995) 1623–1638, [http://dx.doi.org/10.1016/0890-6955\(95\)00014-O](http://dx.doi.org/10.1016/0890-6955(95)00014-O).
- [36] F. Pierron, A. Vautrin, Measurement of the in-plane shear strengths of unidirectional composites with the Iosipescu test, *Compos. Sci. Technol.* 57 (1998) 1653–1660, [http://dx.doi.org/10.1016/S0266-3538\(97\)00099-7](http://dx.doi.org/10.1016/S0266-3538(97)00099-7).
- [37] R. Varadarajan, S.K. Malhotra, L. Vijayaraghavan, R. Krishnamurthy, Mechanical and machining characteristics of GF/PP and GF/Polyester composites, *Mater. Sci. Eng. B* 132 (2006) 134–137, <http://dx.doi.org/10.1016/J.MSEB.2006.02.010>.
- [38] H. Hocheng, H.Y. Puw, Machinability of fiber-reinforced thermoplastics in drilling, *J. Eng. Mater. Technol.* 115 (1993) 146, <http://dx.doi.org/10.1115/1.2902148>.
- [39] H. Hocheng, H.Y. Puw, On drilling characteristics of fiber-reinforced thermoset and thermoplastics, *Int. J. Mach. Tool Manufact.* 32 (1992) 583–592, [http://dx.doi.org/10.1016/0890-6955\(92\)90047-K](http://dx.doi.org/10.1016/0890-6955(92)90047-K).

- [40] F. Quadrini, E.A. Squeo, V. Tagliaferri, Machining of glass fiber reinforced polyamide, *Express Polym. Lett.* 1 (2007) 810–816, <http://dx.doi.org/10.3144/expresspolymlett.2007.112>.
- [41] J. Sheikh-Ahmad, *Machining of Polymer Composites*, Springer US, Boston, MA, 2009, <http://dx.doi.org/10.1007/978-0-387-68619-6>.
- [42] J. Sheikh-Ahmad, J.P. Davim, *Cutting and machining of polymer composites*, Wiley Encycl. Compos, John Wiley & Sons, Inc, Hoboken, NJ, USA, 2012, pp. 648–658, <http://dx.doi.org/10.1002/9781118097298.weoc061>.
- [43] S.K. Chowdhury, A.D. Nimbarte, M. Jaridi, R.C. Creese, Discrete wavelet transform analysis of surface electromyography for the fatigue assessment of neck and shoulder muscles, *J. Electromyogr. Kinesiol.* 23 (2013) 995–1003, <http://dx.doi.org/10.1016/j.jelekin.2013.05.001>.
- [44] M. El Mansori, S. Mezghani, L. Sabri, H. Zahouani, On concept of process signature in analysis of multistage surface formation, *Surf. Eng.* 26 (2010) 216–223, <http://dx.doi.org/10.1179/174329409X455412>.
- [45] M. El Mansori, S. Mezghani, H. Zahouani, F. Divo, Biomimetic touch perception of edge finish of ophthalmic lens, *Wear* 301 (2013) 362–369, <http://dx.doi.org/10.1016/j.wear.2013.01.010>.
- [46] J.P. Davim, P. Reis, Damage and dimensional precision on milling carbon fiber-reinforced plastics using design experiments, *J. Mater. Process. Technol.* 160 (2005) 160–167, <http://dx.doi.org/10.1016/j.jmatprotec.2004.06.003>.
- [47] S. Kherad-Pajouh, O. Renaud, An exact permutation method for testing any effect in balanced and unbalanced fixed effect ANOVA, *Comput. Stat. Data Anal.* 54 (2010) 1881–1893, <http://dx.doi.org/10.1016/j.csda.2010.02.015>.
- [48] D.L. Massart, B.G. Vandeginste, L.M.C. Buydens, S. De Jong, P. Lewi, J. Smeyers-Verbeke, *Handbook of Chemometrics and Qualimetrics: Part A, Data Handl*, Elsevier B.V., Amsterdam, 1998.